# Direct-Drive Wind Generator Concept with Non-Rare-Earth PM Flux Intensifying Stator and Reluctance Outer Rotor

Ali Mohammadi, Oluwaseun A. Badewa, Yaser Chulaee, Dan M. Ionel,
Somasundaram Essakiappan[1], and Madhav Manjrekar[1]

SPARK Laboratory, ECE Department, University of Kentucky, Lexington, KY, USA
[1]QM Power, Inc., Kansas City, MO, USA

alimohammadi@uky.edu, o.badewa@uky.edu, yaser.chulaee@uky.edu, dan.ionel@ieee.org,
somasundaram@qmpower.com, mmanjrekar@qmpower.com

*Abstract*—**This paper proposes a novel concept for an electric generator in which both ac windings and permanent magnets (PMs) are placed in the stator. Concentrated windings with a special pattern and phase coils placed in separate slots are employed. The PMs are positioned in a spoke-type field concentrating arrangement, which provides high flux intensification and enables the use of lower remanence and energy non-rare earth magnets. The rotor is exterior to the stator and has a simple and robust reluctance-type configuration without any active electromagnetic excitation components. The principle of operation is introduced based on the concept of virtual work with closed-form analytical airgap flux density distributions. Initial and parametric design studies were performed using electromagnetic FEA for a 3MW direct-drive wind turbine generator employing PMs of different magnetic remanence and specific energy. Results include indices for the goodness of excitation and the goodness of the electric machine designs; loss; and efficiency estimations, indicating that performance comparable to PM synchronous designs employing expensive and critical supply rare-earth PMs may be achieved with non-rare earth PMs using the proposed configuration.**

*Index Terms*—**Direct-drive generator, wind turbine, electric machine, FEA, spoke permanent magnets, flux-intensifying topology, toroidal winding.**

## I. Introduction

Over the last decade, the offshore wind generation industry has grown annually by approximately 25% on average. In recent years, the development and deployment of offshore wind technology contributed around 10% to the worldwide wind industry with the market share predicted to double by 2025 [1]. Countries across the world are currently evaluating and planning for the potential energy available through offshore wind generation. For example, a previous study found that widespread installation throughout the North Sea would generate enough electricity to satisfy the energy requirements of the EU [2]. Towards a future 100% sustainable future, the continued technological development of wind turbine technology may enable greater energy generation potential at a lower material cost.

Wind turbine manufacturers have undergone significant technological development to enable higher power level operation from 50kW in the 80's to typical ratings of starting around 2 to 3MW today [2]. Wind turbines comprise an electric generator and an associated power electronic converter. In traditional turbines, a multi-stage gearbox is employed to adapt the slow turbine speed to a generator compatible synchronous speed [3], [4].

The gearbox has been reported as one of the most expensive components of offshore wind turbines that may be associated with failures and the resulting operational downtime [5]. Recent studies including around 350 offshore wind turbines found that the gearbox has to be replaced approximately every 6.5 years, a substantially shorter lifespan than the 20 years expected of the turbine generator [6]. In addition, the gearbox contributes to the losses in the drive train [4].

Gear-less or direct-drive generator systems in which the turbine shaft is directly connected to the generator rotor have been proposed and developed to mitigate the aforementioned issues. The simplification of the system through gearbox removal is reported to result in potentially higher efficiency and greater reliability [7].

Due to the high torque needed at low speed, direct-drive generators are substantially larger in size and more expensive than geared equivalents [4], [8], [9].

High specific torque PM synchronous machines have been developed for servo drives and traction applications, e.g. [11], [12], [13]. Special structured topologies such as PM assisted synchronous reluctance machines with V-shape PMs [14] are promising for flux concentration and the vernier type axial flux configuration have shown promise for direct-drive low-speed applications such as wind turbine generators. Vernier type machines with concentrated windings provide greater magnetic flux concentration through high rotor polarities and can ease manufacturing as they require less stator coils than conventional distributed windings [15]. Offshore wind turbines require increased reliability compared to onshore counterparts, prompting wind turbine manufacturers to consider more reliable direct-drive PM synchronous generators [8].

A summary of the dimensions and performance of exam-

| Ref. | Power [MW] | Airgap dia. [m] | Stack length [m] | Eff. [%] | Total losses [kW] | Specific PM mass [g/Nm] | Specific total mass [g/Nm] | Specific thrust [kN/m2] | Goodness [kNm/$\sqrt{W_{loss}}$] |
|------|-----------|----------------|-----------------|---------|------------------|------------------------|---------------------------|------------------------|-----------------------------------|
| [4]  | 3.0 | 4.7 | 1.2 | 96.0 | 125 | 0.895 | 12.684 | 44.864 | 5.374 |
| [10] | 3.1 | 5.0 | 1.9 | 97.2 | 86  | 1.793 | N/A    | 26.537 | 6.620 |
| [10] | 3.0 | 5.0 | 1.9 | 95.9 | 128 | 1.451 | N/A    | 25.867 | 5.622 |

ple PM synchronous generator designs for direct-drive wind turbines is provided in Table I. The electric machines have approximately the same power rating and all of them employ rare earth NdFeB type PM. The cost of materials is therefore expected to be higher, especially when the application is the very large diameter wind turbines that require a large volume of rare-earth PMs. It is important to note that NdFeB, results in a high airgap flux density, however, the large volume of PM in these generators also increases the manufacturing difficulties due to the extremely high forces between PMs. The uncovered references only partially disclose the data of these generator designs, therefore not supporting a detailed comparative study. The efficiency reported in Table I is calculated based on the information provided in the references.

In this paper, the novel concept proposed for a direct-drive generator is inspired from a topology introduced by the research group in a previous paper [16]. In the new approach, the PMs that are placed in the stator, are positioned in a spoke-type arrangement, which greatly intensifies the flux and hence enables the use of relatively low specific energy non-rare-earth PMs. The paper includes parametric studies based on 2D electromagnetic FEA, a procedure for sizing the PMs and for selecting the magnet grade, and example designs evaluated on multiple performance criteria.

## II. THE TOPOLOGY AND OPERATION PRINCIPLE OF THE PROPOSED GENERATOR

The proposed generator has a special configuration, as shown in Fig. 1. The stator has multiple sections, each including a PM and a single concentrated coil belonging to a phase winding. The stator core is modular and with rectangular slots that enable the use of rectangular wire leading to a high slot fill factor and low copper losses. The concentrated coils are toroidally wound with compact axial ends, providing further contribution in reducing copper losses. The winding pattern follows the succession of the three phases around the stator circumference and high fault tolerance is achieved by placing only one coil side in each slot.

The PMs are also placed in the stator, in a radial position, and each two consecutive PMs are magnetized tangentially in opposite directions. It should be noted that the magnets can substantially extend in the radial direction enabling very high flux concentration and achieving flux airgap flux densities considerably higher than the remanence of the PM.

The rotor does not include any active excitation components and has a laminated steel core of the reluctance-type with protrusions, the number and dimensions of which are coordinated with the stator characteristics.
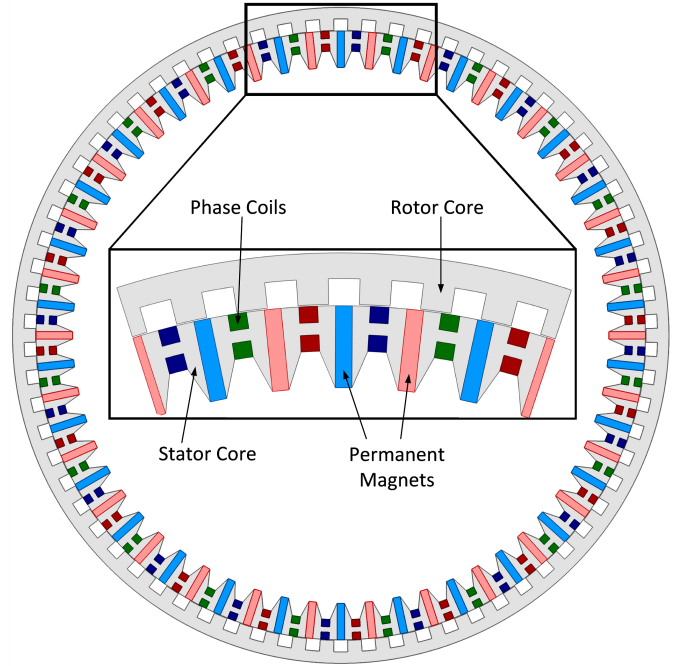


Figure 1. Cross-section and enlarged detailed view of the proposed generator concept. The example design has 60 double stator slots, 3-phase toroidal winding with concentrated coils, and 70 rotor protrusions corresponding to 140 magnetic poles.
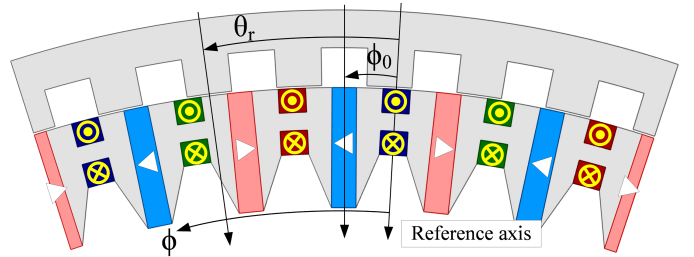


Figure 2. Cross-section of the smaller periodicity region for the example generator design with 7 rotor protrusions. The noted angular coordinates as indicated are used in the analysis of the machine. The reference axis is middle of the stator slots.

The studied minimal region of periodicity is illustrated in Fig. 2 within the proposed concept and has 7 rotor protrusions, operating in a generator with an equivalent of 14 magnetic poles. This region was repeated 10 times to produce 140 magnetic poles. To explain the working principle of the proposed generator concept and the torque generation mechanism, the open-circuit (OC) PM field and the armature field are analyzed using the MMF-permeance model depicted in Fig. 3.

To study the OC PM field, the armature windings are not considered, leaving only the PMs as the source of the magnetic field [16]. Without taking into account the stator's slotting effect, the airgap flux density distribution produced by PMs can be calculated with:

$$
\begin{aligned}
B_{PM}(\varphi,t) = & \\
& F_{PM}P_{PM}\frac{\Lambda_{avg}}{\kappa_{PM}}\,\sin\left(\kappa_{PM}\left(\phi-\phi_0\right)\right)+ \\
& F_{PM}P_{PM}\frac{\Lambda_{pp}}{4\kappa_{PM}}\sin\left(\kappa_{PM}+N_{pr}\right)\cdot \\
& \left[\phi-\frac{N_{pr}\omega_r t-\kappa_{PM}\phi_0-N_{pr}\theta_r}{\kappa_{PM}+N_{pr}}\right]+ \\
& F_{PM}P_{PM}\frac{\Lambda_{avg}}{\kappa_{PM}}\sin\left(\kappa_{PM}-N_{pr}\right)\cdot \\
& \left[\phi+\frac{N_{pr}\omega_r t+\kappa_{PM}\phi_0-N_{pr}\theta_r}{\kappa_{PM}-N_{pr}}\right],
\end{aligned}
\tag{1}
$$

where, $B_{PM}(\phi,t)$ is the flux density distribution in the airgap due to PMs; $F_{PM}$ the amplitude of the square-wave MMF created by PMs; $\Lambda_{avg}$ the average of the maximum and minimum of the airgap permeance; $P_{PM}$ half of the number of PMs; $\phi$ the mechanical angle alongside the peripheral of the airgap with its initial position with respect to the reference axis $\phi_0$; $\kappa_{PM}$ is equal to $(2k+1)P_{PM}$ and $k$ is a positive integer; $N_{pr}$ the number of rotor protrusions, $\omega_r$ the mechanical speed of the rotor, and $\theta_r$ and t are the rotor initial position and time, respectively. Considering only the PMs as the source of magnetic flux, according to (1), there are three groups of flux density harmonics with different rotational speeds and respective pole pairs of $\kappa_{PM}$, $\kappa_{PM}+N_{pr}$ and $|\kappa_{PM}-N_{pr}|$.

The distribution of airgap flux density as a result of disregarding the PMs and only considering the armature winding $B_{AR}(\phi,t)$ [15], can also be similarly obtained:

$$
\begin{aligned}
B_{AR}(\varphi,t) = & \left(\frac{3}{\pi}\right)W_{max}I_m\Lambda_{avg}\cdot \\
& \sum_m^{\infty}\left(\frac{P_{AR}}{m}\right)\sin m\left[\phi-\phi_{a0}-\left(\frac{\omega t-\phi_a}{m}\right)\right]+ \\
& \left(\frac{3}{4\pi}\right)W_{max}I_m\Lambda_{pp}\sum_m^{\infty}\left(\frac{P_{AR}}{m}\right)\sin\left(m+N_{pr}\right)\cdot \\
& \left[\phi-\frac{\omega t+\varphi_a-m\phi_{a0}-(N_{pr}\omega_r)(t+1)}{m+N_{pr}}\right]+ \\
& \left(\frac{3}{4\pi}\right)W_{max}I_m\Lambda_{pp}\sum_m^{\infty}\left(\frac{P_{AR}}{m}\right)\sin\left(m-N_{pr}\right)\cdot \\
& \left[\phi-\frac{\omega t+\varphi_a-m\phi_{a0}+(N_{pr}\omega_r)(t+1)}{m-N_{pr}}\right],
\end{aligned}
\tag{2}
$$

where, $B_{AR}(\phi,t)$ is the distribution of airgap flux density resulting solely from the armature windings; $W_{max}$ and $I_m$ are the saw-tooth wave winding function and phase current peak values, respectively; $P_{AR}$ is the number of coils per phase in the armature winding; variables $m$, $r$, and $t$ are positive integers, and $m = 3r+1 = tP_{AR}$; $\omega$ is the
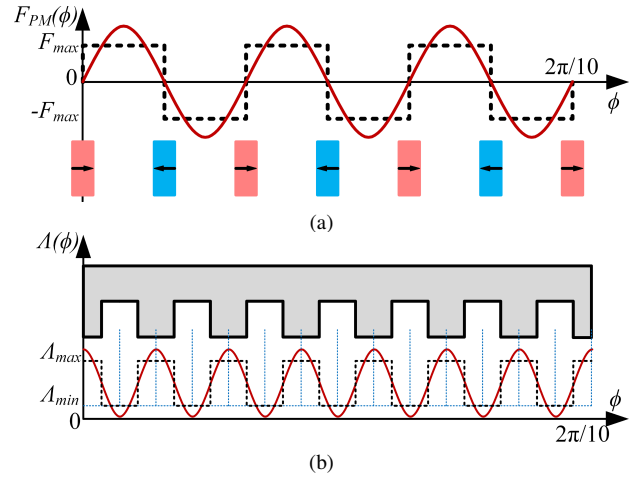


Figure 3. Schematic of an MMF-permeance model for the proposed generator with PM only (a), and with armature windings and airgap permeance ($\Lambda$).

electrical frequency; $\phi_a$ the phase angle relative to $\phi_{a0}$ from the reference axis to the winding axis with three groups of flux density harmonics with $m$, $m+N_{pr}$, and $|m-N_{pr}|$ pole pairs.

Adjacent PMs are magnetized in the opposite direction of one another, which is illustrated in Fig. 3(a); providing flux intensification. The overall electromagnetic performance of the machine is determined by the combination of stator PMs, rotor protrusions and stator toroidal coils layout. The electromagnetic torque can be obtained using the principle of virtual work with the closed-form analytical airgap flux density distributions of PMs, $B_{PM}(\phi,t)$, and armature windings, $B_{AR}(\phi,t)$, and can be expressed by:

$$
\begin{aligned}
T_{emg} &= \frac{\partial W_{co}}{\partial \theta_r} = \frac{\partial}{\partial \theta_r}\int_V \frac{B(\phi,t)^2}{2\mu_0}\mathrm{d}V \\
&= \frac{D_s g\ell_{stk}}{4\mu}\frac{\partial}{\partial \theta_r}\int_0^{2\pi}\left[B_{PM}(\phi,t)+B_{AR}(\phi,t)\right]^2\mathrm{d}\phi,
\end{aligned}
\tag{3}
$$

where, $D_s$ is the stator outer diameter, $g$ the airgap length, and $\ell_{stk}$ the machine axial stack length. By using the orthogonal properties of sinusoidal behavior, it can be inferred that only the dominant airgap flux density harmonics from the PM and armature fields with pole pairs of 4, 6, 8, 16, 18, and 28 would create a non-zero average electromagnetic torque in the example generator.

The suitable combinations of stator PMs, rotor protrusions, and stator winding patterns that provide non-zero average torque can be derived by analyzing (3). The designs with 5, and 7 protrusions with a stator including 6 PMs and 6 toroidal coils, and the designs with 10, and 14 and seven protrusions with a stator including 12 PMs and 12 toroidal coils, are typical topologies produced from this method. The proposed topology explored herein has 70 rotor protrusions and 60 stator PM and toroidal coil, that are a set of the possible working combinations of rotor protrusions, stator PMs, and coils, which must be multiples of 14 and 12, respectively.
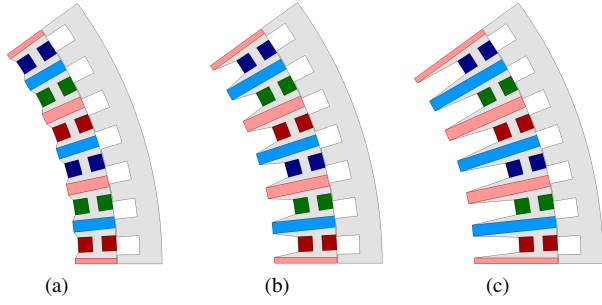
Figure 4. Example proposed designs for flux concentration ratios of (a) two, (b) three, and (c) four.

## III. DESIGN CONSIDERATIONS AND NUMERICAL STUDIES

For low-speed direct-drives typically the best suited are machines with a large number of poles, a short core length, and a relatively large diameter [12]. The airgap flux density for a spoke PM arrangement can be estimated by:

$$B_{ag} = B_r \left( \frac{\pi D_g}{4k_\sigma p h_{PM}} + \frac{2\mu_r g}{\ell_{PM}} \right)^{-1}, \qquad (4)$$

where, $D_g$ is the airgap diameter, $p$ the number of pole pairs, $\mu_r$ the PM relative permeability, $B_r$ the PM remanent flux density, and $k_\sigma$ the rotor leakage coefficient, which can be adjusted to account for the saturation and slotting effects; the PM length in the direction of magnetization is $\ell_{PM}$ and the PM height along the rotor radius is $h_{PM}$. The airgap flux density is directly proportional to the PM remanent flux density, its length, and height. For a fixed value of PM length and height, the airgap flux density variation with PM remanent flux density can be shown as Fig. 5. It should be noted that in this figure, the airgap flux densities are shifted to have a better visibility. The flux density and flux lines for the example design with PM remanent flux density of 0.4T is shown in Fig. 6, and it shows that saturation is heavily present, even with ferrite PMs.

The flux concentration ratio of $\xi$, can be defined based on the length of the PMs by:

$$\xi = \frac{2h_{PM}}{\tau_p}, \qquad (5)$$

where, $\tau_p$ is the stator pole pitch, i.e., stator outer circumference $\pi D_s$ divided by the number of PMs $n_{PM}$. It should be noted that the spoke type topology is particularly beneficial in high polarity machines like the proposed concept in this paper due to the flux concentration effect wherein the magnetic flux of two magnets contributes to the airgap magnetic flux in each pole [12], [11]. Different flux concentration ratios can be achieved and Fig. 4 depicts the proposed topology concept with flux concentration ratios of two, three and four.

In order to decide on a suitable flux concentration ratio, the concept of "excitation goodness" is defined as the ratio of the flux on magnet surface per magnet mass and is calculated as:

$$GD_{exc} = \frac{h_{PM} B_{PM} \ell_{stk}}{M_{PM}}, \qquad (6)$$
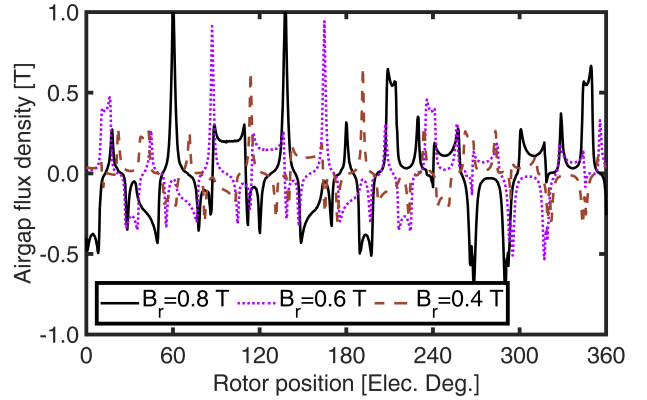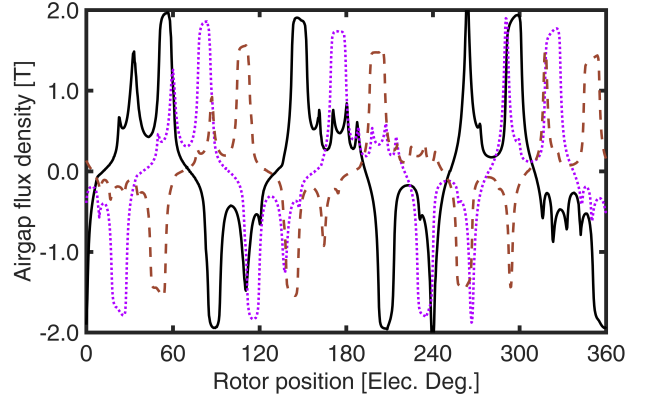


Figure 5. The airgap flux density of the proposed generator concept with three different PMs, with remanent flux densities of 0.4T, 0.6T, and 0.8T (a) the radial component of flux density, and (b) the tangential component of flux density, respectively.

where, $B_{PM}$ and $M_{PM}$ are the average flux density and mass for each PM respectively, which are calculated by performing 2D electromagnetic finite element analysis employing the ANSYS Electronics Desktop software [17]. The airgap flux density and excitation goodness versus flux concentration ratio for the PMs with a remanent flux density of 0.4T are shown in Fig. 7, where, the base value for excitation goodness is equal to 1.38mWb/kg. By increasing the flux concentration ratio from 2 to 4, excitation goodness decreases, raising the PM weight and airgap flux density. Considering excitation goodness and airgap flux density, a flux concentration ratio of 3 is suitable for a 0.4T PM remanent flux density. Similarly, by employing PMs with a remanent flux density of 0.8T, a flux concentration ratio of 3 is also a suitable choice, as demonstrated in Fig. 8, where, the excitation goodness base value is 3.09mWb/kg.

Using the electromagnetic torque and the square root of total losses, the goodness of the machine is defined as:

$$GD = \frac{T_{emg}}{\sqrt{W_{loss}}}, \qquad (7)$$

The total loss for this generator includes components in the laminated core, and winding copper, calculated as:
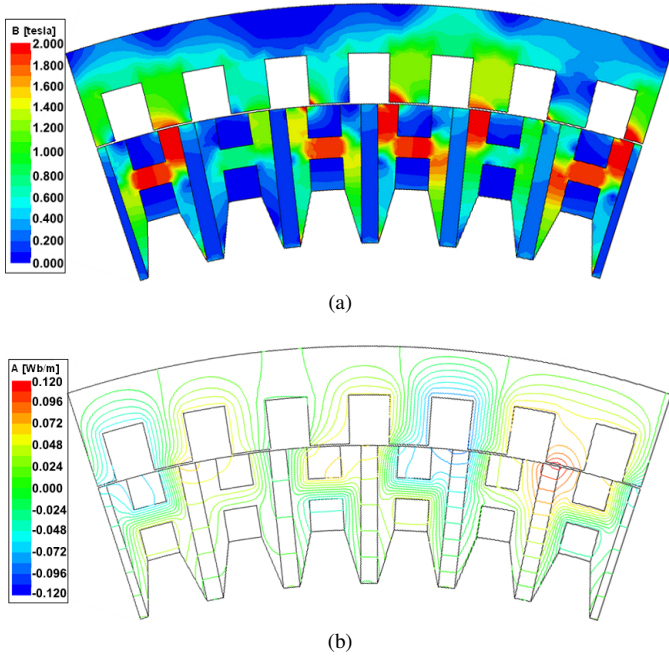
(a)



(b)

Figure 6. (a) Flux density, and (b) flux lines of the proposed generator concept with PM remanent flux density of 0.4T, the flux concentration ratio of three and PM width to stator pole pitch ratio of 0.2.

$$W_{loss} = P_{Cu} + P_{edy} + P_{Fe}$$
$$= 3R_{ph}I_{ph}^2 + P_{edy} + \sum \left[ P_h\left(B, f\right) + P_e\left(B, f^2\right) \right], \quad (8)$$

where, the winding resistance and current per phase are $R_{ph}$, and $I_{ph}$, respectively and $P_{edy}$ the eddy current losses in the winding. Core losses include hysteresis $P_h$ and eddy current losses $P_e$, both as a function of frequency $f$ and magnetic flux density $B$. The calculated copper loss is constant regardless of the flux concentration and PM width to stator pole pitch ratios, because the analysis is performed at constant electrical loading. In the analysis reported in this paper the winding supplementary eddy current losses $P_{edy}$, have been neglected.

The goodness of the proposed concept at different flux concentration, and PM width to stator pole pitch ratios, is depicted in Fig. 9 for two different PMs with remanent flux densities of 0.4T, and 0.8T. Considering the variation of the machine goodness at different flux concentration ratios, 0.2 is considered to be a suitable ratio for PM width to stator pole pitch.

## IV. DISCUSSION

An example generator design with flux concentration ratio of 3, and PM width to stator pole pitch ratio of 0.2, was further studied. The energy stored in a PM is calculated as:

$$W_m = V_m \frac{B_r^2}{2\mu_0\mu_r} \quad (9)$$

where, $V_m$ is the PM volume, and $\mu_0$ the vacuum relative permeability. The specific energy of PM can be defined as
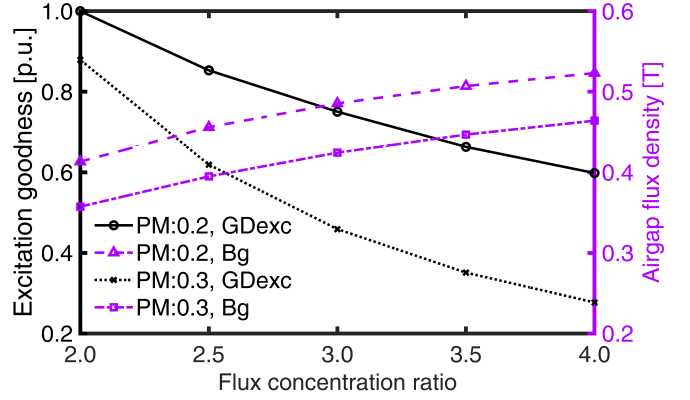


Figure 7. Excitation goodness and absolute average airgap flux density at open-circuit for different ratios of PM width in the magnetization direction to stator pole pitch (as shown in the legend by PM:0.2, and PM:0.3) and different flux concentration ratios for ferrite with remanent flux density of 0.4T.
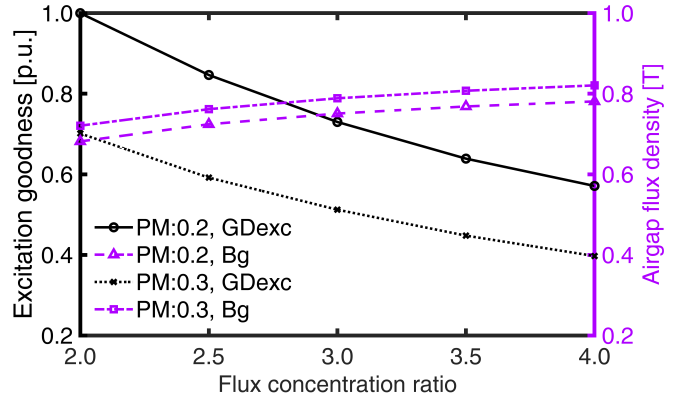


Figure 8. Excitation goodness and absolute average airgap flux density at open-circuit for different ratios of PM width in the magnetization direction to stator pole pitch (as shown in the legend by PM:0.2, and PM:0.3) and different flux concentration ratios for ferrite with remanent flux density of 0.8T.
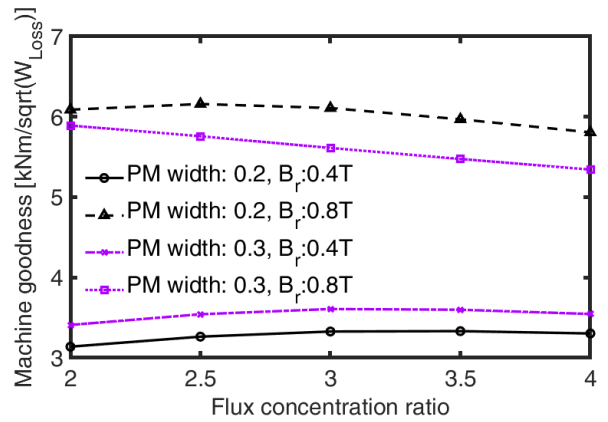


Figure 9. Machine goodness for flux concentrations of 2 to 4 and two different values for the PM width ratio to stator pole pitch.

the amount of energy stored in PMs per unit of volume. The proposed concept design uses a typical ferrite with a remanent flux density of 0.4T and the goodness of the machine is approximately half of the goodness of the machines reported with NdFeB. The ferrite has a remanent flux density, approximately 3 times lower than rare-earth type NdFeB, which can be correlated with one order of magnitude less specific energy. Employing a PM with remanent flux density of only 0.8T that is approximately 40% less than the remanent of NdFeB, leads to the goodness value comparable with much more expensive machines with rare-earth PMs, owing to the high flux concentrating concept of this paper.

A specific torque constant for a machine with given slot and winding may be defined as:

$$k_T = \frac{T_{emg}}{J}, \tag{10}$$

where, $J$ is the copper current density of the winding. For remanent flux densities of 0.4T, 0.6T, and 0.8T; the value of $k_T$ is 0.679, 0.919, and 1.088MNm/(A/mm$^2$), respectively; with the non-linear effect being caused by magnetic saturation.

## V. Conclusion

The new concept of a direct-drive wind turbine electric generator, which was proposed in the paper, is advantageous as it employs a simple and robust reluctance-type outer rotor configuration and an inner stator with 3-phase special windings and PMs in an arrangement that intensifies the magnetic flux. An initial sizing procedure for the dimensions of the PMs and the selection of their material characteristics has been introduced. The approach is based on the concept of goodness of excitation in order to ensure the efficient utilization of PMs. Based on a dimensional and parametric study that considered non-rare earth PMs with a remanent flux density between 0.4T and 0.8T, and focused on the machine goodness index, it can be concluded that designs based on the proposed topology can achieve comparable performance to their conventional counterparts employing NdFeB.

## Acknowledgment

## References

[1] "Global offshore wind report 2020," *GWEC: Brussels, Belgium*, vol. 19, pp. 10–12, 2020.
[2] F. Blaabjerg and D. M. Ionel, "Renewable energy devices and systems – state-of-the-art technology, research and development, challenges and future trends," *Electric Power Components and Systems*, vol. 43, 2015.
[3] G. Shrestha, H. Polinder, D. Bang, and J. Ferreira, "Review of energy conversion system for large wind turbines," in *2008 European wind energy conference, EWEC, Brussels, Belgium.* EWEA, 2008, pp. 1–10.
[4] H. Polinder, F. F. Van der Pijl, G.-J. De Vilder, and P. J. Tavner, "Comparison of direct-drive and geared generator concepts for wind turbines," *IEEE Transactions on Energy Conversion*, vol. 21, no. 3, pp. 725–733, 2006.
[5] A. K. Papatzimos, T. Dawood, and P. R. Thies, "Data insights from an offshore wind turbine gearbox replacement," vol. 1104, no. 1, 2018.
[6] J. Carroll, A. McDonald, and D. McMillan, "Failure rate, repair time and unscheduled O&M cost analysis of offshore wind turbines," *Wind Energy*, vol. 19, no. 6, pp. 1107–1119, 2016.
[7] K. Ahsanullah, R. Dutta, and M. Rahman, "Review of PM generator designs for direct-drive wind turbines," in *2012 22nd Australasian Universities Power Engineering Conference (AUPEC)*, 2012, pp. 1–6.
[8] R. S. Semken, M. Polikarpova, P. Röyttä, J. Alexandrova, J. Pyrhönen, J. Nerg, A. Mikkola, and J. Backman, "Direct-drive permanent magnet generators for high-power wind turbines: Benefits and limiting factors," *IET Renewable Power Generation*, vol. 6, no. 1, pp. 1–8, 2012.
[9] Z. Zhang, A. Chen, A. Matveev, R. Nilssen, and A. Nysveen, "High-power generators for offshore wind turbines," *Energy Procedia*, vol. 35, pp. 52–61, 2013.
[10] M. Lehr, D. Dietz, and A. Binder, "Electromagnetic design of a permanent magnet flux-switching-machine as a direct-driven 3MW wind power generator," in *2018 IEEE International Conference on Industrial Technology (ICIT)*, 2018, pp. 383–388.
[11] D. M. Ionel, J. Eastham, and T. Betzer, "Finite element analysis of a novel brushless dc motor with flux barriers," *IEEE Transactions on magnetics*, vol. 31, no. 6, pp. 3749–3751, 1995.
[12] D. M. Ionel, D. Jackson, G. Starr, and A. Turner, "Permanent magnet brushless motors for industrial variable speed drives," in *2002 International Conference on Power Electronics, Machines and Drives (Conf. Publ. No. 487)*. IET, 2002, pp. 650–654.
[13] A. Fatemi, D. M. Ionel, M. Popescu, Y. C. Chong, and N. A. Demerdash, "Design optimization of a high torque density spoke-type PM motor for a formula E race drive cycle," *IEEE Transactions on Industry Applications*, vol. 54, no. 5, pp. 4343–4354, 2018.
[14] A. Mohammadi and S. M. Mirimani, "Design of a novel pm-assisted synchronous reluctance motor topology using V-shape permanent magnets for improvement of torque characteristic," *IEEE Transactions on Energy Conversion*, vol. 37, no. 1, pp. 424–432, 2021.
[15] M. G. Kesgin, P. Han, D. Lawhorn, and D. M. Ionel, "Analysis of torque production in axial-flux vernier PM machines of the magnus type," in *2021 IEEE International Electric Machines & Drives Conference (IEMDC)*. IEEE, 2021, pp. 1–5.
[16] P. Han, M. G. Kesgin, D. M. Ionel, R. Gosalia, N. Shah, C. J. Flynn, C. S. Goli, S. Essakiappan, and M. Manjrekar, "Design optimization of a very high power density motor with a reluctance rotor and a modular stator having PMs and toroidal windings," in *2021 IEEE Energy Conversion Congress and Exposition (ECCE)*. IEEE, 2021, pp. 4424–4430.
[17] *Ansys® Electronics, version 21.2, 2021, ANSYS Inc.*